

Article

Selective Separation of Arsenic from Lead Smelter Flue Dust by Alkaline Pressure Oxidative Leaching

Wei Liu ¹, Zihan Li ¹, Junwei Han ^{1,2,*}, Wenhua Li ¹, Xun Wang ¹, Na Wang ¹ and Wenqing Qin ^{1,2}

¹ School of Minerals Processing and Bioengineering, Central South University, Changsha 410083, China; liuweipp1@126.com (W.L.); lizihan_kmust@163.com (Z.L.); liwenhua6630@163.com (W.L.); q652617345@163.com (X.W.); wangna2706@163.com (N.W.); qinwenqing369@126.com (W.Q.)

² Key Laboratory of Hunan Province for Clean and Efficient Utilization of Strategic Calcium-containing Mineral Resources, Central South University, Changsha 410083, China

* Correspondence: hanjunwei@csu.edu.cn; Tel.: +86-0731-88879622

Received: 25 April 2019; Accepted: 15 May 2019; Published: 18 May 2019



Abstract: This study investigated the feasibility of using an alkaline pressure oxidative leaching process to treat lead smelter flue dust containing extremely high levels of arsenic with the aim of achieving the selective separation of arsenic. The effects of different parameters including NaOH concentration, oxygen partial pressure, liquid-to-solid ratio, temperature, and time for the extraction of arsenic were investigated based on thermodynamic calculation. The results indicated that the leaching efficiency of arsenic reached 95.6% under the optimized leaching conditions: 80 g/L of NaOH concentration, 1.0 MPa of oxygen partial pressure, 8 mL/g of liquid-to-solid ratio, 120 °C of temperature, 2.0 h of time. Meanwhile, the leaching efficiencies of antimony, cadmium, indium and lead were less than 4.0%, basically achieving the selective separation of arsenic from lead smelter flue dust. More than 99.0% of arsenic was converted into calcium arsenate product and thus separated from the leach solution by a causticization process with CaO after other metal impurities were removed from the solution with the addition of Na₂S. The optimized causticization conditions were established as: 4.0 of the mole ratio of calcium to arsenic, temperature of 80 °C, reaction time of 2.0 h. The resulting product of calcium arsenate may be used for producing metallic arsenic.

Keywords: alkaline pressure oxidative leaching; selective arsenic removal; causticization; lead smelter flue dust; purification

1. Introduction

The smelting utilization of lead concentrate, which is processed in the pyrometallurgical process, produces huge quantities of flue dust with a considerable amount of various elements, such as Pb, Cu, Fe, As, Cd, Sb, Zn, Bi, and Ag [1]. Arsenic is the main unfavorable element of concern in the dust, and is getting more and more attention with the improvement of public awareness of environmental protection due to its toxicity, volatility, bioaccumulation in the environment, and potential carcinogenic propensities [2]. During the smelting process, the main part of the total input of arsenic from the lead concentrate is eliminated through the gas phase, subsequently creating lead smelter flue dust [3].

The high content of arsenic not only effectively reduces the economic value of lead smelter flue dust due to requirements for further operations of hazardous emissions, but also creates great risks to the environment and the human body [4,5]. Arsenic has been classified as a Group 1 human carcinogen by the international agency for research on cancer, and arsenic exposure is associated with an increased incidence of human malignancies in skin, lungs, bladder, and liver [6–8]. As mentioned above, although arsenic in nature has many negative effects, there is still value and necessity in

recycling it due to its current uses, where it is applied in the manufacture of glasses, lead additives in car batteries, anti-friction agents in bearings and Gallium-Arsenide (GaAs) semiconductors [9,10].

Additionally, with respect to the rich metal elements of lead smelter flue dust, the dust is regarded as a secondary resource, which should be properly disposed of and comprehensively utilized to avoid pollution of the ecological environment and to achieve the maximum economic benefits [11,12]. At present, the methods for the comprehensive utilization of lead smelter flue dust can be divided into pyrometallurgical and hydrometallurgical processes. Pyrometallurgical processes mainly include reduction roasting, volatilization roasting and eliminating arsenic in vacuum, and hydrometallurgical processes mainly include acid leaching and alkaline leaching [13,14]. In pyrometallurgical processes, the removal of the arsenic from the smelter flue dust is mainly carried out by calcination. When the temperature reaches 465 °C or higher, arsenic trioxide (As_2O_3) in the dust will violently volatilize into the flue gas, while arsenic will be separated from other high boiling point or non-volatile materials. The pyrometallurgical process is relatively simple and widely used. However, due to the low boiling point of As_2O_3 , most arsenic and arsenic oxide can easily evaporate during the pyrometallurgical processes, which results in metal dispersion, high energy consumption and secondary pollution [15]. Compared with pyrometallurgical processes, hydrometallurgical processes are more environmentally friendly and thus gradually become an important research direction for the treatment of smelter flue dust. Arsenic has obvious dispersibility during acid leaching process, which increases the difficulty of separating arsenic from other valuable metal elements in the leachate [16,17]. In contrast, alkaline solution is selective in dissolving arsenic and has a significantly faster leaching rate than acid leaching, which is because arsenic oxides and arsenates are readily soluble in an alkaline medium [18]. For alkaline leaching, sodium hydroxide (NaOH) or sodium hydroxide-sodium sulfide (NaOH and Na_2S) is usually employed as the leaching agent.

The alkaline pressure oxidative leaching (APOL) process is an effective method for arsenic extraction and has been widely studied for the treatment of wastes containing arsenic. Liu et al. [19] proposed the APOL process to selective extract arsenic from copper anode slime with the leaching efficiency of arsenic reaching up to 99.0%. Han et al. [20] pretreated the tin anode slime by the APOL and obtained great leaching rates of 92.2% tin and 96.5% arsenic, respectively. He et al. [14] developed a pressure oxidative leaching process in NaOH– $NaNO_3$ leaching system to dispose the lead anode slime with the arsenic leaching rate reaching the highest value of 95.9%. Yu et al. [21] used the same technology to separate arsenic from the cobalt and nickel slag with the extraction rate of arsenic reaching 99.1%. However, there are few reports on the removal of arsenic from lead smelter flue dust with extremely high arsenic using the APOL process, up to now.

In the present study, a cleaning process including the steps of the APOL, purification of leachate and causticization with calcium oxide (CaO) was developed to selectively extract arsenic from lead smelter flue dust, while also obtaining calcium arsenate ($Ca_3As_2O_8$) product for use in producing metallic arsenic. Firstly, the Eh–pH diagram of As– H_2O system was established to guide the leaching experiments. The effects of NaOH concentration, oxygen partial pressure, liquid-to-solid ratio (L/S), temperature and time on the leaching efficiencies of arsenic and antimony were investigated in detail. The effects of different parameters including CaO dosage, temperature and time on the causticization process were also investigated. The characterization of solid samples, which include original material, leach residue and precipitate are analyzed by X-ray powder diffraction (XRD) and scanning electron microscopy associated with energy dispersive spectrometry (SEM-EDS). The chemical analyses of both solid and solution samples are analyzed by inductively coupled plasma emission spectrometer (ICP). Please note that all analyses of experimental samples are to confirm the experimental results and revealing some mechanism. The objective of this work is to develop a highly efficient, easy to handle, economical and eco-friendly technology for the preparation of calcium arsenate from lead smelter flue dust, which is crucial for the control of arsenic pollution in the environment and has potential application in producing metallic arsenic.

2. Materials and Methods

2.1. Materials

The powder sample of the dust used in this study was obtained from a lead smelter (Hunan, China). The high-arsenic dust (As > 30 wt. %) could not be recirculated back into the smelting system and converting process [22]. The original dust was firstly dried at 100 °C for 24 h in a draught drying cabinet and then crushed, ground and mixed to a homogeneous powder for the preparation of analytical and experimental samples [23,24]. The main chemical composition of the high-arsenic dust is given in Table 1. As can be seen, the high-arsenic dust contained up to 34.2% arsenic and a certain amount of valuable metals, making it essential to remove the arsenic in advance for preventing secondary pollution and recycling resource. The XRD pattern of the sample shown in Figure 1 indicates that the phase of arsenic in the high-arsenic dust was mainly in the form of As_2O_3 . The phase of lead was mainly in the form of lead (II) chloride fluoride (PbClF), and no other apparent mineral phase could be identified in the high-arsenic dust due to the amorphous nature and the relatively low content. The SEM images of the original materials and the chemical composition determined by EDS are presented in Figure 2. It was apparent that the As_2O_3 existed in cubic crystal and the result of the EDS pattern with the corresponding area in Figure 2d was basically consistent with the results analyzed by XRD.

Table 1. Main chemical composition of the high-arsenic dust.

Composition	As	Cl	Pb	O	Sb	Cd	Zn
wt. %	34.20	14.10	11.10	9.35	7.36	6.63	5.66
Composition	Ca	S	Sn	In	F	Bi	Else
wt. %	5.00	3.28	1.06	0.73	0.73	0.20	0.60

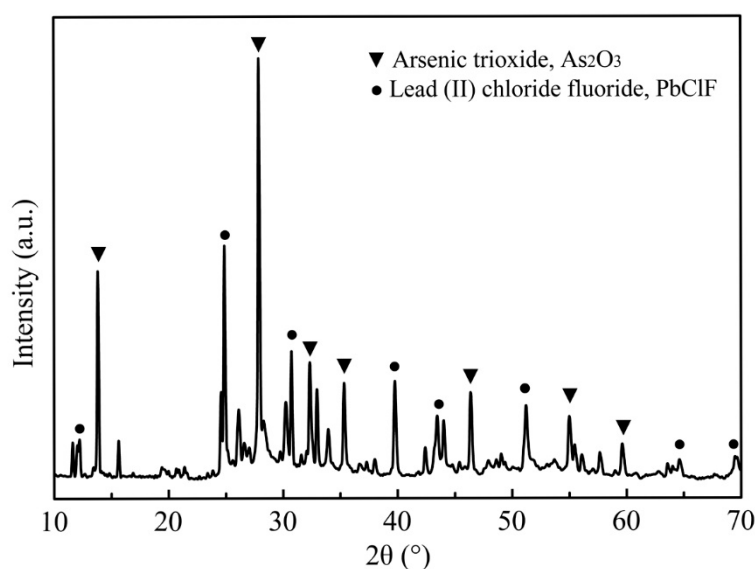


Figure 1. XRD pattern of the high-arsenic dust.

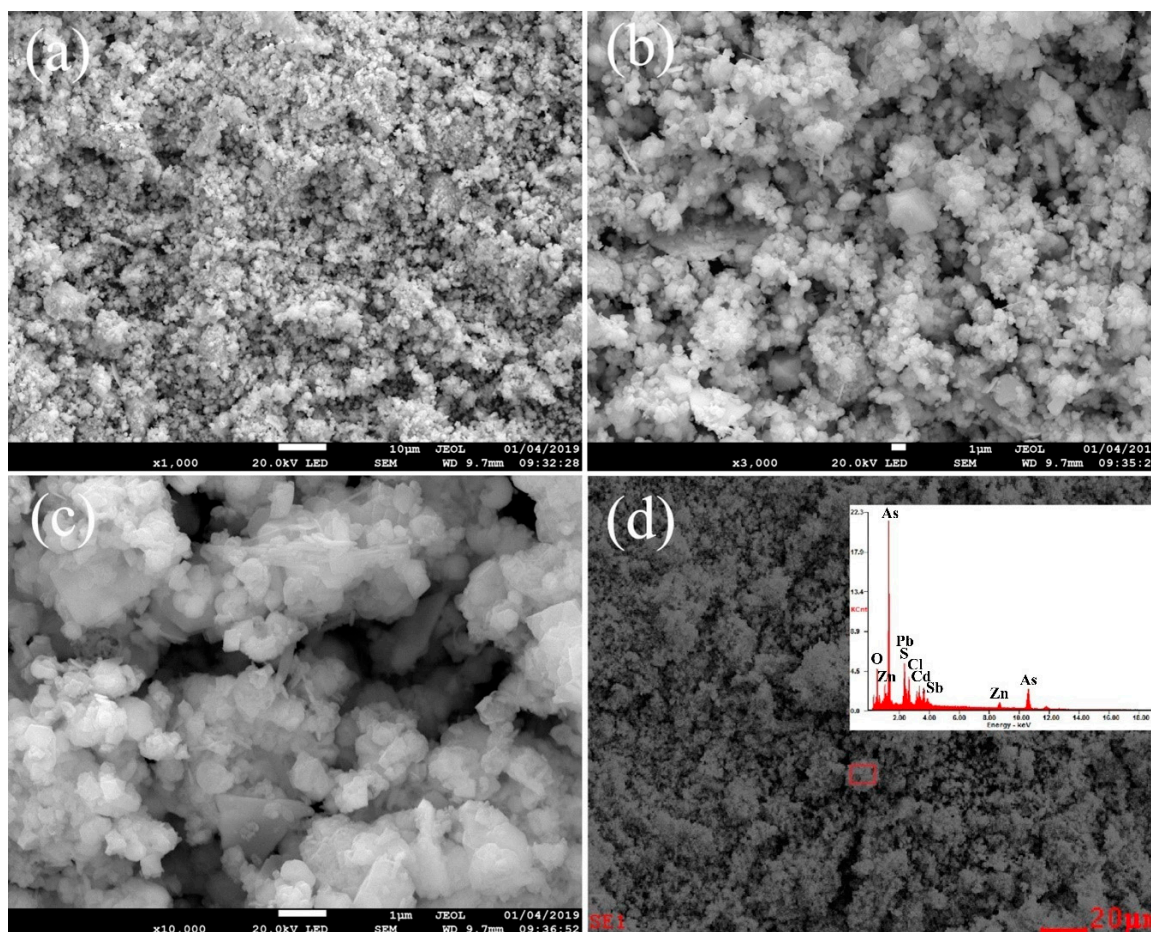


Figure 2. SEM images of the high-arsenic dust at 1000 times magnification (a), 3000 times magnification (b), and 10,000 times magnification (c); and EDS pattern with the corresponding area (d).

2.2. Experimental Setup and Procedure

An experimental schematic diagram of the proposed process is presented in Figure 3. The experiments of the APOL were conducted in an autoclave, which consisted of a kettle body, a kettle cover, a stirring motor, a heater, a cooling system and an electric control cabinet. The oxygen tank was used as an accessory device to provide stable and continuous oxygen partial pressure. The kettle body and the kettle cover were made of stainless steel, and a pressure gauge was placed on the kettle cover. Temperature, voltage, time, stirring speed and switches of the autoclave were controlled by the electric control cabinet. For each test, 50 g of the high-arsenic dust and NaOH solution with the scheduled liquid-to-solid ratio and concentration were firstly mixed and poured into the autoclave, which had been washed with NaOH solution. Then the autoclave was sealed and heated under stirring at 220 V, and the cooling water of the stirring motor was also turned on. When heating to the desired temperature, the main valve and the partial pressure valve of the oxygen tank were opened to control the pressure inside the autoclave. After the required leaching time had been reached, the heating function and the inlet valve were turned off, and the cooling water was fed into the cooling system to cool the autoclave to about 70–80 °C. At the end of each experiment run, the slurry in the autoclave was pumped after opening the kettle cover and vacuum filtrated to separate the solids from the solution. The filtrate was measured for volume using a measuring cylinder and sampled for chemical composition by ICP. The remaining leach residue was washed with deionized water several times and then dried, weighed, and ground, followed by digestion and chemical composition analysis.

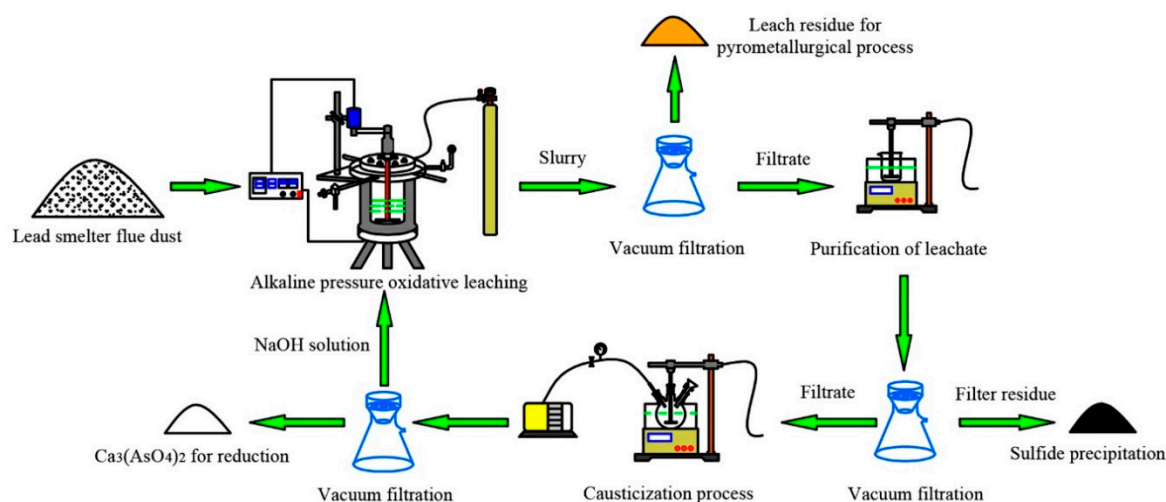


Figure 3. The experimental schematic diagram of the proposed process.

After other metal impurities were removed from the leachate with the addition of Na_2S [25], the purified leachate was then subjected to the causticization process, which was performed to precipitate arsenic with CaO powder in a flask with three necks. At the end of the causticization experiment, the slurry in the flask was vacuum filtrated, measured for volume, and sampled. The final solution and solid products were then analyzed by ICP, XRD and SEM-EDS.

In addition, all reagents used for experiment and chemical analysis in this study were of analytical grade, including the NaOH used in the leaching, the Na_2S used for purification, the CaO used in causticization, etc. Meanwhile, oxygen (O_2) with 99.9% purity was used in the APOL experiments, and deionized water was prepared through a laboratory water purification system (Medium-1600).

2.3. Analytical Methods

The leaching results were evaluated by chemically determining the original materials and leach products using ICP, XRD and SEM-EDS. The element concentrations of both solid and solution samples were determined by ICP (ICAP7400 Radial, Intrepid II XSP, Waltham, MA, USA), and each sample was measured at least three times [26–28]. 1 mL of leachate was diluted with 500 mL 10% HNO_3 medium to provide a sample with the appropriate concentration. 0.1 g of leach-concentrated hydrochloric acid (HCl) and nitric acid (HNO_3) were placed on a hot plate and diluted with 500 mL 10% HNO_3 medium to provide a sample with the appropriate concentration. The other solid samples were prepared in the same manner, with 10% HNO_3 as the dilution medium to prevent hydrolysis. In addition, the compositions of the original materials and solid samples were analyzed using XRD (Bruker-axs D8 Advance, Karlsruhe, Germany) to observe changes in phase formations [29]. The particle shapes and the elemental compositions were observed by SEM (JEOL, JSM-6490LV, Tokyo, Japan) coupled with EDS (EDAX, NEPTUNE TEXS HP, McKee Drive Mahwah, NJ, USA).

3. Results and Discussion

3.1. Eh–pH Diagram

Eh–pH diagrams show the thermodynamic stability areas of different species in an aqueous solution. Stability areas are presented as a function of pH and electrochemical potential scales. In the present study, the $\text{As-H}_2\text{O}$ system was used as guidance in pH and potential values of the leaching situation. The Eh–pH diagram of the $\text{As-H}_2\text{O}$ system at 120 °C was calculated by HSC Chemistry 6.0. Please note that the concentrations of related ions were fixed at 1 mol/L, and both the partial pressures of oxygen and hydrogen were at the standard atmospheric pressure of 101,325 Pa. Figure 4 shows that

increasing the potential value was beneficial to the conversion of $\text{As} \rightarrow \text{As(III)} \rightarrow \text{As(V)}$. In alkaline solution, the concentration of H^+ is so low that most of As(V) exists as monomeric AsO_4^{3-} [30].

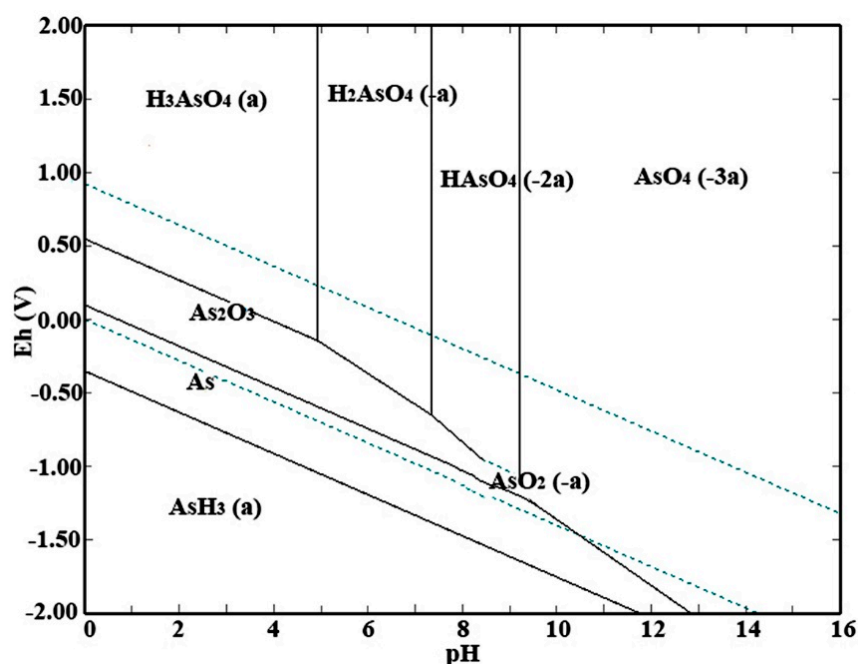


Figure 4. Eh–pH diagram of As–H₂O system at 120 °C.

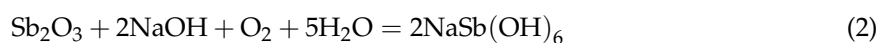
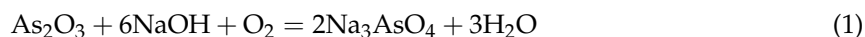
Please note that the dissolution behaviors of arsenic and antimony are similar in a single alkaline leaching system. However, the strong oxidative condition of the APOL process can be used to avoid the leaching of antimony due to the different transformations of arsenic and antimony. In the case of sufficient alkalinity, the low-solubility As_2O_3 can be completely oxidized to AsO_4^{3-} by dissolved O_2 for the conversion of As(III) to As(V) and to form soluble sodium arsenate (Na_3AsO_4), while diantimony trioxide (Sb_2O_3) is transformed into insoluble sodium antimonate hydrate (NaSb(OH)_6) [31].

For other elements, lead, copper, cadmium can be oxidized to soluble species in acid solution and to insoluble species in neutral or alkaline solution. However, excessive hydroxyl ion (OH^-) can slowly dissolve lead, copper, cadmium and their oxides in strong alkaline solution. This means that the proper concentration of NaOH can avoid the leaching of these metals. Zinc and its oxides are soluble both in acid solution and alkaline solution. The contents of bismuth, indium and tin of the high-arsenic dust are extremely low, and these elements are not the main object of the present investigation.

In summary, the Eh–pH diagram of As–H₂O system indicated that a strong alkaline solution and an oxidative environment were essential conditions for the conversion of As_2O_3 to AsO_4^{3-} , while also avoiding the leaching of antimony. That is to say, selective separation of arsenic from lead smelter flue dust by the APOL process is feasible in thermodynamics.

3.2. Alkaline Pressure Oxidative Leaching

The possible reactions of As_2O_3 and Sb_2O_3 in NaOH-O_2 leaching system are expressed as Equations (1) and (2):



The thermodynamic parameters of Equation (1) at different temperatures were calculated as shown in Table 2, which indicated that Equation (1) was thermodynamically feasible.

Table 2. Thermodynamic parameters of Equation (1) at different temperatures.

T/°C	$\Delta H/\text{KJ}$	$\Delta S(\text{J/K})$	$\Delta G/\text{KJ}$
80	−723.85	−50.50	−706.01
100	−722.50	−46.79	−705.04
120	−721.19	−43.36	−704.14
140	−752.32	−121.20	−702.24
160	−751.10	−118.34	−699.85
180	−749.96	−115.81	−697.50

Alkaline leaching is more likely to achieve selective arsenic removal than acid leaching, and the effect of NaOH concentration on the APOL process was firstly investigated under the following conditions: temperature of 120 °C, liquid-to-solid ratio of 8 mL/g, time of 2.0 h, oxygen partial pressure of 1.0 MPa and stirring speed of 250 rpm. Figure 5a illustrates the leaching efficiencies of arsenic and antimony over an alkalinity range from 20 g/L to 100 g/L of NaOH. From the initial NaOH concentration of 20 g/L to 80 g/L, the leaching efficiency of arsenic increased significantly from 62.0% to 98.6%, while the leaching efficiency of antimony gradually decreased from 21.4% to 3.5%. The significant increase in leaching efficiency of arsenic was because more OH[−] reacted with the arsenic of the dust in the same liquid-solid contact surface region, and increased the concentration difference between the surface of the solid particle and the reaction product layer, accelerating diffusion. Meanwhile, the opposite trend for antimony was due to the formation of NaSb(OH)₆ with a low solubility of about 4×10^{-8} [31]. However, a further increase in NaOH concentration had an adverse effect on the leaching of arsenic, resulting in a decrease in the leaching efficiency of arsenic and a slight increase in the leaching efficiency of antimony. When the NaOH concentration was higher than 80 g/L, the leaching efficiency of arsenic decreased to 88.6%. This might be attributed to the high concentration of Na⁺ having a negative influence on the dissolution of arsenate and the reactions between dissolved lead ions and arsenate ions resulting in formation of insoluble compounds. For selective and effective arsenic removal, the optimum NaOH concentration was selected as 80 g/L and applied for all further experiments.

Strong oxidation conditions are one of the important parameters during the APOL process of present study, mainly because O₂ is the key to achieving the oxidative conversion of arsenic from unstable As(III) to stable As(V). The effect of oxygen partial pressure on APOL process was therefore investigated under the following conditions: NaOH concentration of 80 g/L, liquid-to-solid ratio of 8 mL/g, time of 2.0 h, temperature of 120 °C and stirring speed of 250 rpm. The results in Figure 5b illustrate the effect of oxygen partial pressure in the range from 0 MPa to 2.0 MPa on the leaching efficiencies of arsenic and antimony. It can be seen from Figure 5b that when the oxygen partial pressure was increased from 0 MPa to 1.0 MPa, and then to 2.0 MPa, the leaching efficiency of arsenic increased first from 41.7% to 95.4%, and then decreased to 71.2%. The solubility of O₂ in the solution is mainly determined by oxygen partial pressure. Increasing the oxygen partial pressure within a certain range can significantly increase the oxidation efficiency and accelerate the leaching efficiency of arsenic. On the other hand, increasing oxygen partial pressure can promote the positive movement of Equation (2), so the leaching efficiency of antimony gradually decreased with the increase of oxygen partial pressure within the investigated range. When the oxygen partial pressure was higher than 1.0 MPa, the decrease in leaching efficiency of arsenic was possibly due to the insoluble compounds, which was formed by the reaction between dissolved lead ions and arsenate ions. Therefore, in order to obtain a high leaching efficiency of arsenic, 1.0 MPa was determined to be the optimum oxygen partial pressure.

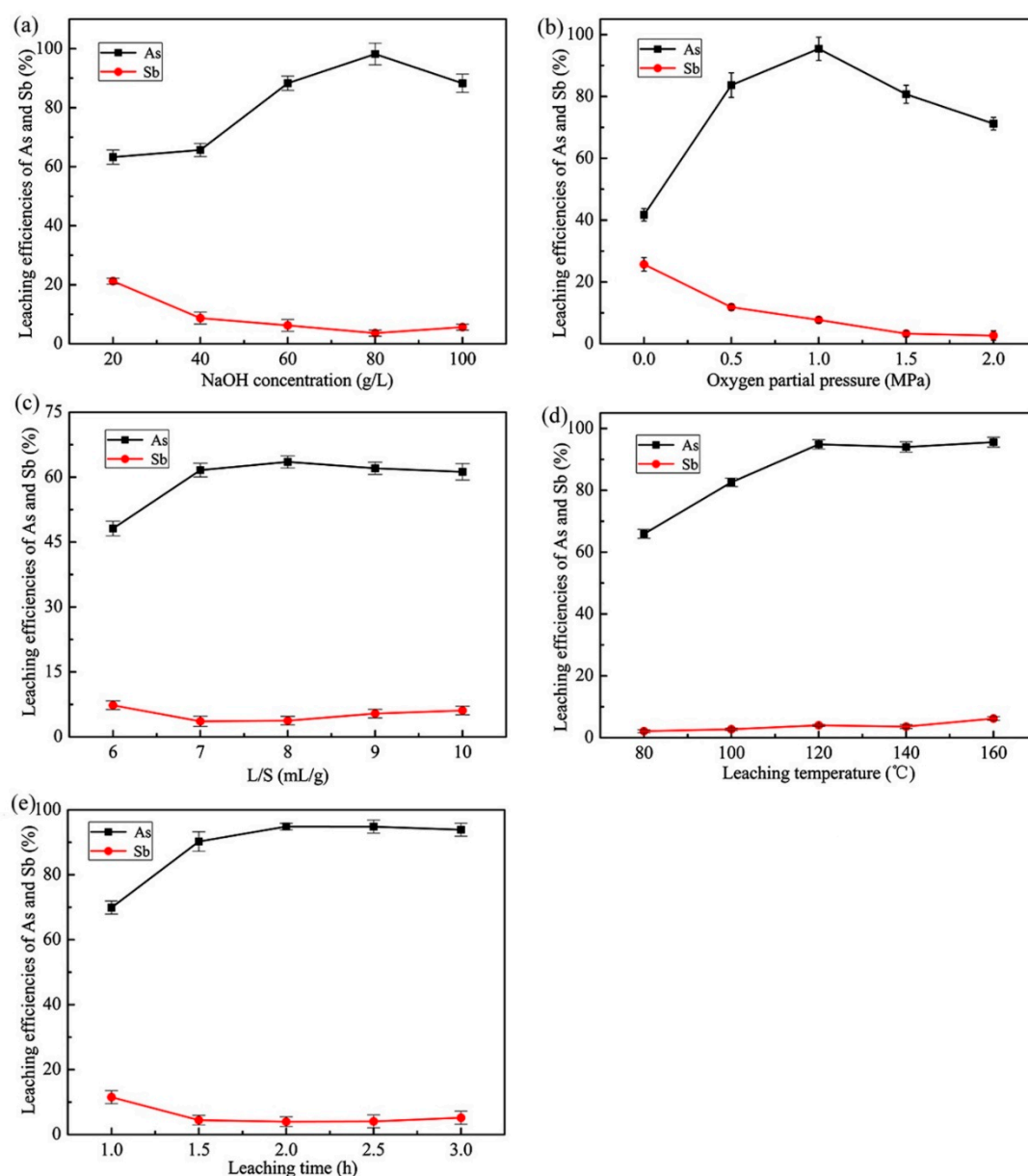


Figure 5. Effects of different APOL conditions on the extractions of As and Sb: (a) NaOH concentration (120 °C, L/S = 8 mL/g, 2.0 h, $pO_2 = 1.0$ MPa, 250 rpm), (b) oxygen partial pressure ([NaOH] = 80 g/L, L/S = 8 mL/g, 2.0 h, 120 °C, 250 rpm), (c) liquid-to-solid ratio ([NaOH] = 80 g/L, 120 °C, 2.0 h, $pO_2 = 1.0$ MPa, 250 rpm), (d) leaching temperature ([NaOH] = 80 g/L, L/S = 8 mL/g, 2.0 h, $pO_2 = 1.0$ MPa, 250 rpm), (e) leaching time ([NaOH] = 80 g/L, L/S = 8 mL/g, 120 °C, $pO_2 = 1.0$ MPa, 250 rpm).

Liquid-to-solid ratio is a crucial technical and economic parameter in the hydrometallurgy leaching process. The effect of the liquid-to-solid ratio on the APOL process was investigated under the following conditions: NaOH concentration of 80 g/L, temperature of 120 °C, time of 2.0 h, oxygen partial pressure of 1.0 MPa and stirring speed of 250 rpm. The results are shown in Figure 5c. As can be seen, the leaching efficiency of arsenic gradually increased from 56.3% to 70.0% when the liquid-to-solid ratio was increased from 6 to 8. After that, the leaching efficiency of arsenic slightly decreased as the liquid-to-solid ratio increased. It was apparent that when a liquid-to-solid ratio of 8 mL/g was used, the efficiencies of extracting arsenic and antimony were the maximum and minimum values within the investigated range, 70.0% and 4.1%, respectively. A suitable liquid-to-solid ratio is an important precondition for obtaining a high leaching efficiency of arsenic. Increasing the liquid-to-solid ratio

under the same NaOH concentration condition is beneficial to sufficiently stirring the solution and reducing the diffusion resistance, and thus obtaining a high leaching efficiency. Therefore, the optimum liquid-to-solid ratio was fixed at 8 mL/g to obtain the maximum leaching efficiency of arsenic.

Leaching temperature is another important factor affecting the leaching process, because the increase of temperature accelerates the chemical reaction kinetics [32]. The effect of leaching temperature on the leaching efficiencies of arsenic and antimony during the APOL process was investigated under the following conditions: NaOH concentration of 80 g/L, liquid-to-solid ratio of 8 mL/g, time of 2.0 h, oxygen partial pressure of 1.0 MPa and stirring speed of 250 rpm. It can be seen from Figure 5d that the leaching efficiency of arsenic increased pronouncedly and gradually reached its maximum of 94.9% with the increase in temperature from 80 °C to 120 °C. Above 120 °C, the leaching efficiency of arsenic showed no significant variations as the temperature increased. Additionally, there was no significant change in the leaching efficiency of antimony in the studied temperature range. Leaching under a high-temperature environment is beneficial to increasing reaction rates, but inevitably leads to greater energy consumption. Therefore, the optimum temperature was determined to be 120 °C to obtain a high leaching efficiency of arsenic while reducing energy consumption. All further experiments were therefore carried out at 120 °C.

The effect of leaching time on the leaching efficiencies of arsenic and antimony during the APOL process was investigated under the following conditions: NaOH concentration of 80 g/L, liquid-to-solid ratio of 8 mL/g, temperature of 120 °C, oxygen partial pressure of 1.0 MPa and stirring speed of 250 rpm. As shown in Figure 5e, the leaching efficiency of arsenic increased significantly from 69.9% to 94.9% in the initial stage of the reaction when the time increased from 1.0 h to 2.0 h, while the leaching efficiency of antimony decreased from 11.5% to 4.0%. The leaching efficiency of arsenic remained almost unchanged with a further increase in time. Suitable leaching time can ensure the high leaching rate and efficiency of the target element. In general, the leaching efficiency is proportional to the leaching time, but the time extension after reaching the diffusion balance will not only reduce production efficiency, but will also result in the leaching of many impurity elements. Considering the maximum selective extraction of arsenic, 2.0 h was selected as the optimum leaching time.

Based on the results of the condition experiments, the optimized conditions of the APOL process were established as: NaOH concentration of 80 g/L, oxygen partial pressure of 1.0 MPa, liquid-to-solid ratio of 8 mL/g, temperature of 120 °C, time of 2.0 h. The optimal experiment was repeated three times, and the results are listed in Table 3. The optimum conditions selected in this study were limited to the specific arsenic content range of raw materials, which aimed to provide theoretical guidance for the treatment of other arsenic-containing materials in the same way. It was found from Table 3 that the results of the three experiments were basically consistent. The average leaching efficiencies of arsenic, antimony, cadmium, indium, lead and zinc were 95.6%, 5.0%, 0.03%, 2.3%, 4.4% and 31.8%, respectively. In addition, the XRD pattern of the leach residue shown in Figure 6 indicated that the main mineral phases were NaSb(OH)₆, lead sulfide (PbS) and cadmium sulfide (CdS), while the apparent mineral phase of As₂O₃ disappeared. The element contents of the leach residue under the optimized conditions are listed in Table 4. This indicated that arsenic in the leach residue was less than 5.0%, and most arsenic entered the leachate, while antimony, cadmium, lead, zinc and other metals were enriched in different degrees in the leach residue. The leach residue could be returned to a pyrometallurgical process to recover valuable elements. The analytical results confirmed that the selective extraction of arsenic was achieved by the APOL process.

Table 3. Leaching efficiencies of confirmation experiments under the optimized conditions (%).

No.	As	Sb	Cd	In	Pb	Zn
I	92.9	3.8	0.02	4.1	3.2	33.2
II	95.4	7.7	0.02	1.4	7.2	34.7
III	98.6	3.5	0.05	1.3	2.9	27.3
Average	95.6	5.0	0.03	2.3	4.4	31.7

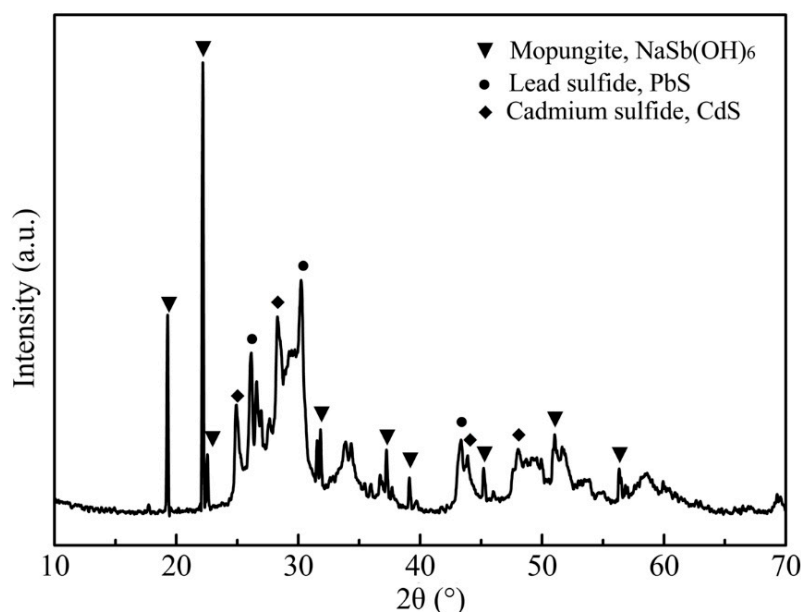


Figure 6. XRD pattern of the leach residue from the APOL process.

Table 4. Main chemical composition of the leach residues with corresponding weights under the optimized conditions (wt. %, g).

No.	As	Sb	Cd	In	Pb	Zn	Weight
I	3.8	15.7	15.6	1.9	26.8	6.5	20.6
II	4.3	14.7	14.8	1.7	26.7	6.7	20.8
III	3.9	13.8	13.7	1.5	24.4	6.5	20.6
Average	4.0	14.7	14.7	1.7	26.0	6.6	20.7

3.3. Purification of Leach Solution

The approach of the APOL process can extract the majority of arsenic from lead smelter flue dust. However, elements such as antimony, cadmium, lead and zinc also partially enter the leachate during the APOL process. To avoid the enrichment of these elements, a metal sulphide precipitation process is performed by adding Na_2S , due to the low solubility of metal sulphide precipitates [33,34]. The purification experiments were conducted under the following conditions: Na_2S solution of 0.5 mol/L, water bath temperature of 30 °C. The results are presented in Table 5. It can be seen that the precipitation rate of arsenic can be controlled to within 10%, while the precipitation rates of lead, zinc and antimony exceed 97.1%, 99.8%, 58.9%, respectively. The deep removal of antimony will be investigated in future research.

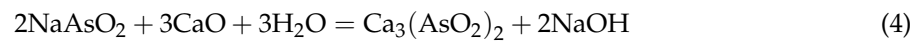
Table 5. Results of purification experiments.

Composition	As	Pb	Sb	Zn
Mixed leachate (g/L)	19.0	0.3	0.06	0.8
Filtrate (g/L)	18.0	0.007	0.02	0.001
Precipitation Rate (%)	9.2	97.1	58.9	99.8

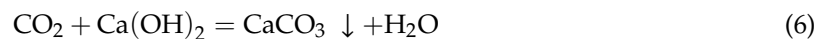
3.4. Causticization Process

A causticization process with CaO powder was performed to obtain calcium arsenate product from the purified leachate [35]. Arsenic is most effectively removed or stabilized when it is presented in the pentavalent arsenate form [36] and arsenic in the alkaline leachate mainly exists in the form of Na_3AsO_4 and sodium arsenite (NaAsO_2). With respect to the safer disposal of the leachate, the causticization

process is applied to remove arsenic by combining arsenate ions with calcium ions to form calcium arsenate or calcium arsenite precipitate. The chemical properties of calcium arsenate are more stable than sodium arsenate and the possible reactions during the causticization process are expressed as Equations (3) and (4):



The causticization process not only reduces the potential hazard of arsenic to the environment, but also produces OH^- to reduce the consumption of alkali medium in the APOL process. CaO dosage, temperature and time are the main parameters affecting the causticization process. To evaluate the removal rate of CaO towards AsO_4^{3-} , the CaO dosage is expressed by the mole ratio of calcium to arsenic (Ca/As). However, it is thought that CO_2 in air may react with the calcium hydroxide solution during the causticization process. The possible reactions of CO_2 are expressed as Equations (5) and (6):



Therefore, the effect of CO_2 on the causticization process was investigated firstly before the condition experiments. The causticization process was carried out in a water bath in air under the following conditions: temperature of 80 °C, time of 2.0 h, Ca/As of 3.0. The XRD pattern of the precipitate shown in Figure 7 indicates that the main mineral phases were calcium hydroxide ($\text{Ca}(\text{OH})_2$), calcium carbonate (CaCO_3) and calcium fluoride arsenate ($\text{Ca}_5\text{F}(\text{AsO}_4)_3$). There is no apparent mineral phase of calcium arsenate identified from the precipitate. There is no doubt that the presence of CO_2 reduces the efficiency of causticization and the purity of the final product. Hence, the effects of different parameters including CaO dosage, temperature and time on the causticization process were investigated in a vacuum to avoid the negative influence of CO_2 .

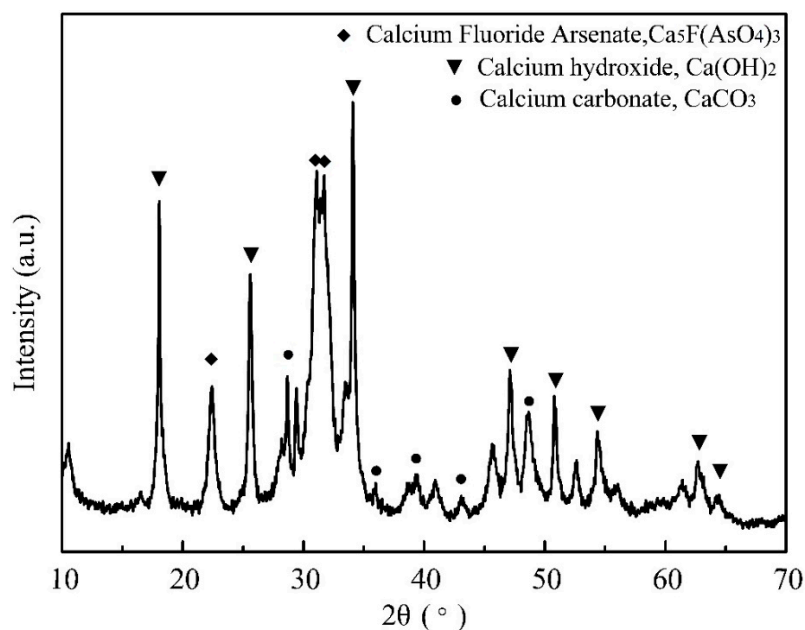


Figure 7. XRD pattern of the precipitate from the causticization process in air.

It is well-known that CaO plays the most important role in the causticization process, because the proper CaO dosage ensures a high precipitation rate of arsenic [12]. The effect of CaO dosage on the

causticization process was investigated under the following conditions: temperature of 80 °C, time of 1.0 h. Figure 8a illustrates the effect of CaO dosage on the precipitation rate of arsenic. It can be seen that the precipitation rate of arsenic increased significantly and reached its maximum of 99.4% when the Ca/As was 4.0. Therefore, 4.0 of Ca/As was determined to be the optimum CaO dosage.

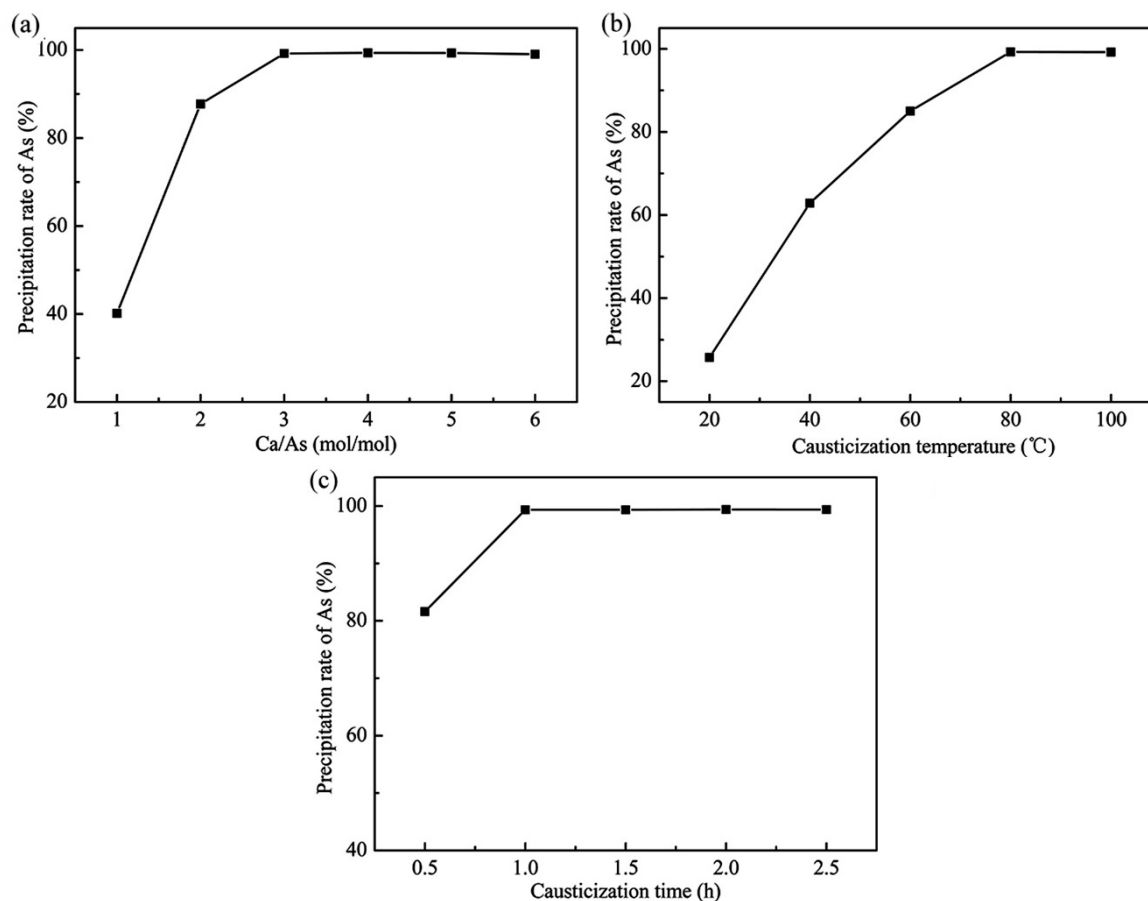


Figure 8. Effects of different causticization conditions on the precipitation rate of As: (a) CaO dosage (80 °C, 1.0 h), (b) causticization temperature (Ca/As = 4, 1.0 h), (c) causticization time (Ca/As = 4, 80 °C).

Temperature is one of the main factors affecting the chemical reaction, and the effect of causticization temperature on the precipitation rate of arsenic was investigated under the following conditions: Ca/As of 4.0, time of 1.0 h. Figure 8b shows the effect of temperature on the precipitation rate of arsenic. It can be seen that the precipitation rate of arsenic increased significantly and gradually reached 99.3% at 80 °C as the temperature increased from 20 °C to 80 °C. The precipitation rate of arsenic remained almost unchanged with the further increase of time. Therefore, 80 °C was selected as the optimum temperature, and all further experiments were performed at 80 °C.

Time is another important factor affecting the chemical reaction, and a suitable time can ensure the high precipitation rate and efficiency. The effect of causticization time on the precipitation rate of arsenic was investigated under the following conditions: Ca/As of 4.0, temperature of 80 °C. The results in Figure 8c illustrate the effect of time in the range from 0.5 h to 2.5 h on the causticization process. At the initial reaction time from 0.5 h to 1.0 h, the precipitation rate of arsenic increased from 81.6% to 99.3%. A further increase in causticization time had almost no effect on the precipitation rate of arsenic. All further experiments were therefore performed for 2.0 h.

According to the results of the condition experiments, the optimized conditions of the causticization process were established as: CaO dosage of 4.0, temperature of 80 °C, time of 2.0 h. Under the optimized experimental conditions, the best precipitation rate of arsenic was 99.4%. The filtrate after causticization

could be returned to the APOL process to realize the recycling of alkali. The chemical composition and XRD analysis of the precipitate are shown in Table 6 and Figure 9. The SEM images of the precipitate and the chemical compositions determined by EDS are presented in Figure 10. As can be seen from Table 6, the main components of the precipitate were 15.1% arsenic and 34.4% calcium. The results analyzed by XRD and the EDS patterns with the corresponding areas in Figure 10c,d indicate that the main phases in the precipitate were $\text{Ca}_5(\text{AsO}_4)_3(\text{OH})$ and $\text{Ca}(\text{OH})_2$, in which $\text{Ca}_5(\text{AsO}_4)_3(\text{OH})$ was the most stable form of calcium arsenate compound. An excessive dosage of CaO can increase the removal rate of arsenic, but inevitably leads to a reduction of $\text{Ca}_5(\text{AsO}_4)_3(\text{OH})$ purity [37]. However, the reduction in the purity of $\text{Ca}_5(\text{AsO}_4)_3(\text{OH})$ does not affect the subsequent reduction experiments for producing metallic arsenic, because $\text{Ca}(\text{OH})_2$ readily decomposes into CaO at a high temperature. The analytical results confirmed that the precipitation of arsenic was achieved by causticization process. The final product of calcium arsenate could be used to produce metallic arsenic by reduction.

Table 6. The chemical analysis of filtrate and precipitate.

Composition	As	Ca
Filtrate (g/L)	0.1	19.8
Precipitate (%)	15.1	34.4

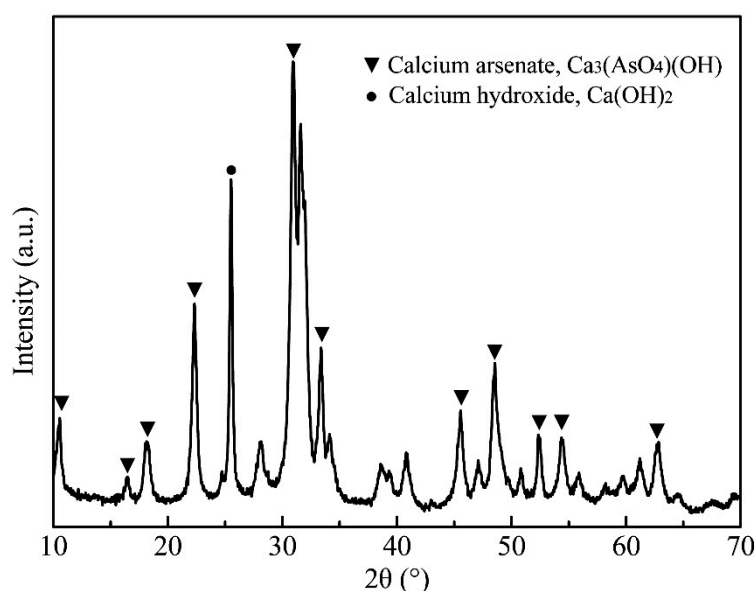


Figure 9. XRD pattern of the precipitate from the causticization process in vacuum.

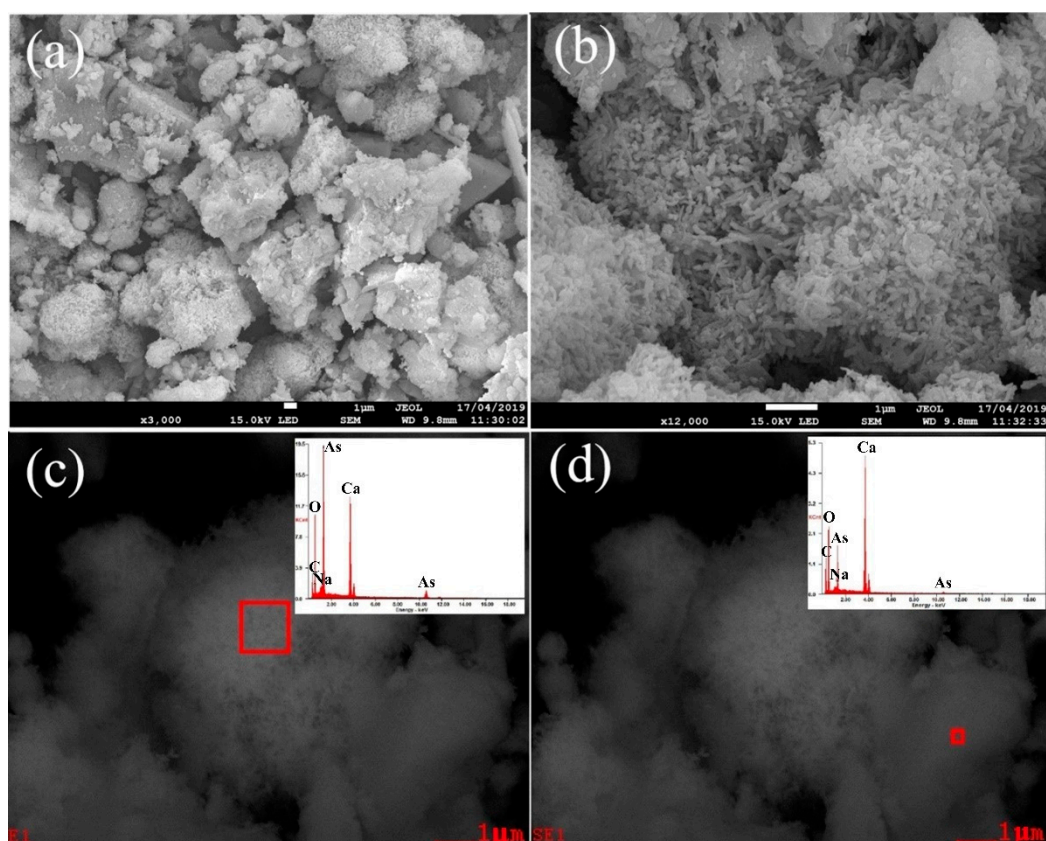


Figure 10. SEM images of the precipitate from the causticization process in vacuum at 3000 times magnification (a), 12,000 times magnification (b), and EDS patterns with corresponding areas at (c) and (d).

3.5. Leaching Toxicity Analysis of the Resulting Product

The discharge of solid wastes is strictly regulated in China, and the identification standards for hazardous waste—Identification for extraction toxicity (GB 5085.3-2007) [38] state that the arsenic concentration permitted for discharge is below 5 mg/L. Consequently, leaching toxicity experiments of starting materials, leach residue and precipitate were conducted according to the solid waste-extraction procedure for leaching toxicity—Sulphuric acid and nitric acid method (HJT299-2007) [39]. The analytical results confirmed that leaching toxicity in the starting material was reduced from 4.05 g/L to 3.78 g/L in the leach residue and then to 10.28 mg/L in the precipitate from the causticization process in vacuum, which demonstrated the feasibility of reducing the leaching toxicity and converting the hazardous waste to general solid waste.

4. Conclusions

About 95.6% of the arsenic was selectively extracted from lead smelter flue dust by alkaline pressure oxidative leaching under optimized conditions: NaOH concentration of 80 g/L, oxygen partial pressure of 1.0 MPa, liquid-to-solid ratio of 8 mL/g, leaching temperature of 120 °C, leaching time of 2.0 h. Meanwhile, the leaching efficiencies of antimony, cadmium, indium, lead and zinc were at low levels. The leach residue could be returned to pyrometallurgical process to recover valuable elements. The metal sulphide precipitation process was performed for purifying other metal impurities of the APOL leachate. After other metal impurities had been removed from the leachate with the addition of Na₂S, more than 99.0% of the arsenic was converted into calcium arsenate product and thus separated from the filtrate by causticization with CaO under optimized conditions: mole ratio of calcium to arsenic of 4.0, temperature of 80 °C, time of 2.0 h. The analytical results by XRD and SEM-EDS indicated

that the arsenic in the dust was converted into $\text{Ca}_5(\text{AsO}_4)_3(\text{OH})$ after the alkaline pressure oxidative leaching, purification and causticization processes. Additionally, the calcium arsenate product will be used for producing metallic arsenic by reduction.

Author Contributions: Conceptualization, W.L. (Wei Liu) and W.Q.; methodology, Z.L. and J.H.; validation, Z.L. and J.H.; formal analysis, Z.L.; investigation, Z.L., X.W. and N.W.; resources, W.L. (Wei Liu) and J.H.; writing—original draft preparation, Z.L., J.H. and W.L. (Wenhua Li); writing—review and editing, J.H.; supervision W.L. (Wei Liu) and J.H.; project administration, W.L. (Wei Liu) and J.H.; funding acquisition, W.Q., W.L. (Wei Liu) and J.H.

Funding: The authors gratefully acknowledge the financial support of the Central South University Graduate Research and Innovation Project (No. 2018zzts793), the National Natural Science Foundation of China (No. 51804342, No. 51874356), the Natural Science Foundation of Hunan Province (2019JJ50805), the Innovation Driven Plan of Central South University (Grant No. 2015CX005), Key Laboratory of Hunan Province for Clean and Efficient Utilization of Strategic Calcium-containing Mineral Resources (No. 2018TP1002), the Scientific Research Starting Foundation of Central South University (No. 218041).

Conflicts of Interest: The authors declare no conflict of interest. The funders had no role in the design of the study; in the collection, analyses, or interpretation of data; in the writing of the manuscript, or in the decision to publish the results.

References

1. Min, X.; Liao, Y.; Chai, L.; Yang, Z.; Xiong, S.; Liu, L.; Li, Q. Removal and stabilization of arsenic from anode slime by forming crystal scorodite. *Trans. Nonferrous Metals Soc. China* **2015**, *25*, 1298–1306. [[CrossRef](#)]
2. Liu, H.; Wang, C.; Zou, C.; Zhang, Y.; Wang, J. Simultaneous volatilization characteristics of arsenic and sulfur during isothermal coal combustion. *Fuel* **2017**, *203*, 152–161. [[CrossRef](#)]
3. Montenegro, V.; Sano, H.; Fujisawa, T. Recirculation of high arsenic content copper smelting dust to smelting and converting processes. *Miner. Eng.* **2013**, *49*, 184–189. [[CrossRef](#)]
4. Liu, R.P.; Yang, Z.C.; He, Z.L.; Wu, L.Y.; Hu, C.Z.; Wu, W.Z.; Qu, J.H. Treatment of strongly acidic wastewater with high arsenic concentrations by ferrous sulfide (FeS): Inhibitive effects of S(0)-enriched surfaces. *Chem. Eng. J.* **2016**, *304*, 986–992. [[CrossRef](#)]
5. Yao, L.; Min, X.; Ke, Y.; Wang, Y.; Liang, Y.; Yan, X.; Xu, H.; Fei, J.; Li, Y.; Liu, D.; et al. Release Behaviors of Arsenic and Heavy Metals from Arsenic Sulfide Sludge during Simulated Storage. *Minerals* **2019**, *9*, 130. [[CrossRef](#)]
6. Zhou, Q.; Xi, S. A review on arsenic carcinogenesis: Epidemiology, metabolism, genotoxicity and epigenetic changes. *Regulat. Toxicol. Pharmacol.* **2018**, *99*, 78–88. [[CrossRef](#)] [[PubMed](#)]
7. Bellamri, N.; Morzadec, C.; Fardel, O.; Vernhet, L. Arsenic and the immune system. *Curr. Opin. Toxicol.* **2018**, *10*, 60–68. [[CrossRef](#)]
8. Inam, A.M.; Khan, R.; Park, R.D.; Ali, A.B.; Uddin, A.; Yeom, T.I. Influence of pH and Contaminant Redox Form on the Competitive Removal of Arsenic and Antimony from Aqueous Media by Coagulation. *Minerals* **2018**, *8*, 574. [[CrossRef](#)]
9. Long, G.; Peng, Y.; Bradshaw, D. A review of copper–arsenic mineral removal from copper concentrates. *Miner. Eng.* **2012**, *36*, 179–186. [[CrossRef](#)]
10. Nazari, A.M.; Radzinski, R.; Ghahreman, A. Review of arsenic metallurgy: Treatment of arsenical minerals and the immobilization of arsenic. *Hydrometallurgy* **2017**, *174*, 258–281. [[CrossRef](#)]
11. Tongamp, W.; Takasaki, Y.; Shibayama, A. Arsenic removal from copper ores and concentrates through alkaline leaching in NaHS media. *Hydrometallurgy* **2009**, *98*, 213–218. [[CrossRef](#)]
12. Hanum, F.F.; Desfitri, R.E.; Hayakawa, Y.; Kambara, S. Preliminary Study on Additives for Controlling As, Se, B, and F Leaching from Coal Fly Ash. *Minerals* **2018**, *8*, 493. [[CrossRef](#)]
13. Chen, Y.; Liu, N.; Ye, L.; Xiong, S.; Yang, S. A cleaning process for the removal and stabilisation of arsenic from arsenic-rich lead anode slime. *J. Clean. Prod.* **2018**, *176*, 26–35. [[CrossRef](#)]
14. He, Y.; Xu, R.; He, S.; Chen, H.; Li, K.; Zhu, Y.; Shen, Q. φ -pH diagram of As–N–Na–H₂O system for arsenic removal during alkaline pressure oxidation leaching of lead anode slime. *Trans. Nonferrous Metals Soc. China* **2017**, *27*, 676–685. [[CrossRef](#)]

15. Jarošíková, A.; Ettler, V.; Mihaljevič, M.; Drahot, P.; Culka, A.; Racek, M. Characterization and pH-dependent environmental stability of arsenic trioxide-containing copper smelter flue dust. *J. Environ. Manag.* **2018**, *209*, 71–80. [[CrossRef](#)]
16. Geveci, A.; Topkaya, Y.; Ayhan, E. Sulfuric acid leaching of Turkish chromite concentrate. *Miner. Eng.* **2002**, *15*, 885–888. [[CrossRef](#)]
17. Kashiwakura, S.; Ohno, H.; Matsubae-Yokoyama, K.; Kumagai, Y.; Kubo, H.; Nagasaka, T. Removal of arsenic in coal fly ash by acid washing process using dilute H₂SO₄ solvent. *J. Hazard. Mater.* **2010**, *181*, 419–425. [[CrossRef](#)] [[PubMed](#)]
18. Awe, S.A.; Sandström, Å. Selective leaching of arsenic and antimony from a tetrahedrite rich complex sulphide concentrate using alkaline sulphide solution. *Miner. Eng.* **2010**, *23*, 1227–1236. [[CrossRef](#)]
19. Liu, W.; Yang, T.; Zhang, D.; Chen, L.; Liu, Y. Pretreatment of copper anode slime with alkaline pressure oxidative leaching. *Int. J. Miner. Process.* **2014**, *128*, 48–54. [[CrossRef](#)]
20. Han, J.; Liang, C.; Liu, W.; Qin, W.; Jiao, F.; Li, W. Pretreatment of tin anode slime using alkaline pressure oxidative leaching. *Sep. Purif. Technol.* **2017**, *174*, 389–395. [[CrossRef](#)]
21. Yu, G.; Zhang, Y.; Zheng, S.; Zou, X.; Wang, X.; Zhang, Y. Extraction of arsenic from arsenic-containing cobalt and nickel slag and preparation of arsenic-bearing compounds. *Trans. Nonferrous Metals Soc. China* **2014**, *24*, 1918–1927. [[CrossRef](#)]
22. Jarošíková, A.; Ettler, V.; Mihaljevič, M.; Penížek, V.; Matoušek, T.; Culka, A.; Drahot, P. Transformation of arsenic-rich copper smelter flue dust in contrasting soils: A 2-year field experiment. *Environ. Pollut.* **2018**, *237*, 83–92. [[CrossRef](#)] [[PubMed](#)]
23. Han, J.; Jiao, F.; Liu, W.; Qin, W.; Xu, T.; Xue, K.; Zhang, T. Innovative Methodology for Comprehensive Utilization of Spent MgO-Cr₂O₃ Bricks: Copper Flotation. *Acs Sustain. Chem. Eng.* **2016**, *4*. [[CrossRef](#)]
24. Han, J.; Liu, W.; Qin, W.; Zhang, T.; Chang, Z.; Xue, K. Effects of sodium salts on the sulfidation of lead smelting slag. *Miner. Eng.* **2017**, *108*, 1–11. [[CrossRef](#)]
25. Feng, Q.; Zhao, W.; Wen, S. Surface modification of malachite with ethanediamine and its effect on sulfidation flotation. *Appl. Surf. Sci.* **2018**, *436*, 823–831. [[CrossRef](#)]
26. Han, J.; Liu, W.; Qin, W.; Peng, B.; Yang, K.; Zheng, Y. Recovery of zinc and iron from high iron-bearing zinc calcine by selective reduction roasting. *J. Ind. Eng. Chem.* **2015**, *22*, 272–279. [[CrossRef](#)]
27. Han, J.; Liu, W.; Qin, W.; Yang, K.; Wang, D.; Luo, H. Innovative methodology for comprehensive utilization of high iron bearing zinc calcine. *Sep. Purif. Technol.* **2015**, *154*, 263–270. [[CrossRef](#)]
28. Han, J.; Liu, W.; Qin, W.; Zheng, Y.; Luo, H. Optimization Study on the Leaching of High Iron-Bearing Zinc Calcine After Reduction Roasting. *Metall. Mater. Trans. Part B* **2016**, *47*, 686–693. [[CrossRef](#)]
29. Han, J.; Liu, W.; Wang, D.; Jiao, F.; Zhang, T.; Qin, W. Selective Sulfidation of Lead Smelter Slag with Pyrite and Flotation Behavior of Synthetic ZnS. *Metall. Mater. Trans. B* **2016**, *47*, 2400–2410. [[CrossRef](#)]
30. Gu, K.; Li, W.; Han, J.; Liu, W.; Qin, W.; Cai, L. Arsenic removal from lead-zinc smelter ash by NaOH-H₂O₂ leaching. *Sep. Purif. Technol.* **2019**, *209*, 128–135. [[CrossRef](#)]
31. Li, Y.; Liu, Z.; Li, Q.; Liu, F.; Liu, Z. Alkaline oxidative pressure leaching of arsenic and antimony bearing dusts. *Hydrometallurgy* **2016**, *166*, 41–47. [[CrossRef](#)]
32. Zhao, H.; Zhang, Y.; Zhang, X.; Qian, L.; Sun, M.; Yang, Y.; Zhang, Y.; Wang, J.; Kim, H.; Qiu, G. The dissolution and passivation mechanism of chalcopyrite in bioleaching: An overview. *Miner. Eng.* **2019**, *136*, 140–154. [[CrossRef](#)]
33. Guo, X.; Yi, Y.; Shi, J.; Tian, Q. Leaching behavior of metals from high-arsenic dust by NaOH-Na₂S alkaline leaching. *Trans. Nonferrous Metals Soc. China* **2016**, *26*, 575–580. [[CrossRef](#)]
34. Lewis, A.E. Review of metal sulphide precipitation. *Hydrometallurgy* **2010**, *104*, 222–234. [[CrossRef](#)]
35. Liu, W.; Li, W.; Han, J.; Wu, D.; Li, Z.; Gu, K.; Qin, W. Preparation of calcium stannate from lead refining slag by alkaline leaching-purification-causticization process. *Sep. Purif. Technol.* **2019**, *212*, 119–125. [[CrossRef](#)]
36. Leist, M.; Casey, R.J.; Caridi, D. The management of arsenic wastes: Problems and prospects. *J. Hazard. Mater.* **2000**, *76*, 125–138. [[CrossRef](#)]
37. Fujita, T.; Taguchi, R.; Shibata, E.; Nakamura, T. Preparation of an As(V) solution for scorodite synthesis and a proposal for an integrated As fixation process in a Zn refinery. *Hydrometallurgy* **2009**, *96*, 300–312. [[CrossRef](#)]

38. Ministry of Environmental Protection of China. *Identification Standards for Hazardous Wastes—Identification for Extraction Toxicity*; GB 5085.3-2007; Ministry of Environmental Protection of China: Beijing, China, 2007. (In Chinese)
39. Ministry of Environmental Protection of China. *Solid Waste-Extraction Procedure for Leaching Toxicity—Sulphuric Acid and Nitric Acid Method*; Ministry of Environmental Protection of China: Beijing, China, 2007. (In Chinese)



© 2019 by the authors. Licensee MDPI, Basel, Switzerland. This article is an open access article distributed under the terms and conditions of the Creative Commons Attribution (CC BY) license (<http://creativecommons.org/licenses/by/4.0/>).